In-band pumped Tm,Ho:LiYF_4 waveguide laser

Pavel Loiko, Esrom Kifle, Gurvan Brasse, Romain Thouroude, Florent Starecki, Abdelmjid Benayad, Alain Braud, Mathieu Laroche, Sylvain Girard, Hervé Gilles, et al.

Research Article | Vol. 30, No. 7 / 28 Mar 2022 / Optics Express 11840
Optics EXPRESS

In-band pumped Tm,Ho:$LiYF_4$ waveguide laser

PAVEL LOIKO, ESROM KIFLE, GURVAN BRASSE, ROMAIN THOUROUDE, FLORENT STARECKI, ABDELMJID BENAYAD, ALAIN BRAUD, MATHIEU LAROCHE, SYLVAIN GIRARD, HERVÉ GILLES, AND PATRICE CAMY*

Centre de Recherche sur les Ions, les Matériaux et la Photonique (CIMAP), UMR 6252 CEA-CNRS-ENSICAEN, Université de Caen Normandie, 6 Boulevard Maréchal Juin, 14050 Caen Cedex 4, France
*patrice.camy@ensicaen.fr

Abstract: A 4.5 at.% Tm, 0.5 at.% Ho:$LiYF_4$ planar waveguide (thickness: 25 μm) grown by Liquid Phase Epitaxy is in-band pumped by a Raman fiber laser at 1679 nm (the $^3H_6 \rightarrow {}^3F_4$ Tm^{3+} transition). A continuous-wave waveguide laser generates a maximum output power of 540 mW at 2051nm with a slope efficiency of 32.6%, a laser threshold of 337 mW and a linear laser polarization (π). This represents the highest output power extracted from any Tm,Ho waveguide laser. No parasitic Tm^{3+} colasing is observed. The waveguide propagation losses are determined to be as low as 0.19 dB/cm.

1. Introduction

Lasers emitting at the wavelengths around 2 μm are attractive for soft material processing, bio- and environmental sensing, spectroscopy and frequency conversion further into the mid-infrared spectral range. Nowadays, there is a trend of laser development towards highly efficient, power scalable and compact (integrated) devices. Waveguide (WG) lasers featuring small mode areas leading to low laser thresholds and high laser intensities, as well as good overlap between the pump and laser modes leading to high slope efficiencies [1], meet these criteria. In particular, continuous-wave and mode-locked 2 μm WG lasers are promising as active element of distributed sensors, as well as compact seed sources for further amplification. Due to their inherently short cavity lengths, in the mode-locked regime of operation, such lasers could deliver ultrashort pulses at high repetition rates (in the GHz-range) [2] which is attractive for the so-called cold ablation of biological tissues [3].

Laser emission slightly above 2 μm is typically achieved using the $^5I_7 \rightarrow {}^5I_8$ electronic transition of Holmium (Ho^{3+}) ions. A common approach for excitation of Ho^{3+} is a codoping of the host matrix by both Tm^{3+} and Ho^{3+} ions. The former ions act as sensitizers and efficiently transfer the energy of electronic excitation to the latter ions, $Tm^{3+}(^3F_4) \rightarrow Ho^{3+}(^5I_7)$, Fig. 1(a). Tm^{3+} ions, in their turn, can be excited at 0.8 μm (into the $^3H_4$ pump level), e.g., by AlGaAs diode lasers, representing a conventional pumping scheme. Efficient continuous-wave bulk Tm,Ho lasers are known [4,5]. The main disadvantage of this pump scheme is a significant heat release due to (i) the non-radiative path from the $^3H_4$ and $^3H_5$ Tm^{3+} excited-states, (ii) parasitic energy-transfer upconversion (ETU) from the metastable states of both Tm^{3+} and Ho^{3+} ions, and (iii) energy loss due to the back energy transfer. The heating leads to severe thermo-optic effects even at moderate pump levels causing a thermal roll-over in the output dependence, laser ceasing or even crystal fracture. It is probably because of this reasons that the development of Tm,Ho WG lasers was not very intense so far [6–8]. Lancaster *et al.* reported on a Tm,Ho:ZBLAN glass WG fabricated by femtosecond direct laser writing (DLW) and delivering only 76 mW at 2052nm with a moderate slope efficiency of 20% [6].

#449126 https://doi.org/10.1364/OE.449126
Journal © 2022 Received 18 Nov 2021; revised 28 Jan 2022; accepted 1 Feb 2022; published 24 Mar 2022

Optics EXPRESS

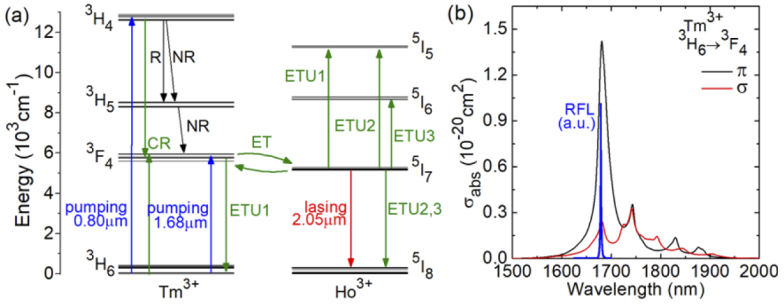

Fig. 1. (a) The scheme of energy levels of Tm^{3+} and Ho^{3+} ions in $LiYF_4$ showing pump (*blue*) and laser (*red*) transition, ET – energy-transfer, CR – cross-relaxation, ETU – energy-transfer upconversion, R and NR – radiative and non-radiative relaxation, respectively; (b) absorption cross-sections, σ_{abs}, for the $^3H_6 \rightarrow {}^3F_4$ transition of Tm^{3+} ions in $LiYF_4$ for π and σ polarizations, the spectrum of the Raman fiber laser (*blue*) is shown for comparison.

An alternative pumping scheme of Tm^{3+},Ho^{3+}-codoped materials is the direct excitation of Tm^{3+} ions to the $^3F_4$ state (the so-called Tm in-band pumping), Fig. 1(a). It may greatly reduce the energy losses originating from the non-radiative path of Tm^{3+} ions. Such approach has been studied recently for both bulk [9] and WG [10] lasers based on singly Tm^{3+}-doped materials showing good prospects for both achieving high slope efficiency and power scaling. Loiko *et al.* reported on an in-band pumped Tm:$LiYF_4$ WG fabricated by Liquid Phase Epitaxy (LPE) generating a record-high output power of 2.05 W at 1881nm with a high slope efficiency of 78.3% [10]. Note that the in-band pumping of Tm^{3+} ions around 1.6–1.7 μm is feasible based on the well-developed Er fiber laser technology. It should be noted that singly Ho^{3+}-doped materials can also be in-band pumped (directly to the $^5I_7$ state), e.g., by Tm bulk or fiber lasers emitting at ~1.9 μm. In-band pumped Ho WG lasers have been reported [11,12]. The advantage of Tm^{3+},Ho^{3+} codoped materials as compared to singly Ho^{3+}-doped ones (even if both are in-band pumped) is the combined gain bandwidth of both ions around 2 μm supporting broader range of wavelength tuning and the generation of shorter pulses in the mode-locked regime [13].

First in-band pumped bulk and WG Tm,Ho lasers were reported recently. Kalachev *et al.* used a Raman-shifted Er fiber laser to pump a Tm,Ho:$LiYF_4$ crystal yielding an output power of 400 mW at 2052nm with a high slope efficiency of 44% [14]. Kifle *et al.* applied a similar pump source for a Tm,Ho:$KLu(WO_4)_2$ WG laser fabricated by DLW; however, the authors detected parasitic Tm^{3+} colasing limiting the power scaling capabilities for Ho^{3+} radiation [15].

In the present work, we report on a power-scalable Tm,Ho waveguide laser operating solely on the $^5I_7 \rightarrow {}^5I_8$ Ho^{3+} transition and based on the Tm in-band pumping scheme which mitigates the thermal effects and provides a relatively high slope efficiency. We have used a Tm,Ho:$LiYF_4$ planar WG fabricated by LPE to benefit from good thermal properties of this fluoride host material.

2. Experimental

2.1. Planar waveguide

Single-crystalline layers of RE:$LiYF_4$ (where RE = Gd, Tm and Ho) were grown by Liquid Phase Epitaxy. Bulk undoped $LiYF_4$ substrates with their surfaces parallel to the (001) crystallographic plane were used. The substrates were cut from a boule grown by the Czochralski method. They were double side polished with small surface roughness (few nm). For LPE, the batch composition was 73 mol% LiF – 27 mol% REF_3 (RE = Y, Gd, Tm, Ho). LiF was used as a

Optics EXPRESS

solvent. The growth was performed in pure Ar atmosphere. The growth temperature was ~734 °C and its duration was 45 min.

The optically passive Gd^{3+} ions (3.5 at.% in the layer) were intentionally added to enhance the refractive index contrast between the layer and the substrate ($\Delta n = n_{layer} - n_{substrate} = 2\times10^{-3}$, $n_{substrate} = 1.4445$ at the wavelength of ~2 μm for π-polarization). The actual doping levels of laser-active ions (in the layer) were 4.5 at.% Tm and 0.5 at.% Ho, and the corresponding ion densities amounted to $N_{Tm} = 6.2\times10^{20}$ at/cm^3 and $N_{Ho} = 0.70\times10^{20}$ at/cm^3, respectively.

The top surface of the epitaxy was polished resulting in a layer thickness of 25 ± 1 μm, see Fig. 2. The input and output faces were polished as well and left uncoated. The planar WG sample was oriented for light propagation along the ***a***-axis (***a***-cut) and its length t was 8.0 mm.

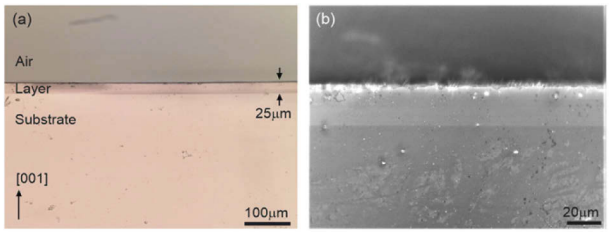

Fig. 2. Observation of a polished side facet of the Tm,Ho:$LiYF_4$ / $LiYF_4$ epitaxy: (a) optical microscope, crossed polarizers, ×10 objective; (b) confocal laser microscope, UV illumination, ×100 objective.

2.2. Laser set-up

The scheme of the laser set-up is shown in Fig. 3(a). The bottom (substrate) part of the epitaxy was mounted on a passively cooled Cu-holder using a silver paint for better heat removal. The laser cavity was formed by two plane mirrors: a pump mirror (PM) coated for high transmission ($T = 93\%$) at 1.68 μm and for high reflectance (HR) at 1.86–2.32 μm, and a set of plane output couplers (OCs) with a transmission T_{OC} at the laser wavelength in the range of 1.5% - 30%. Both cavity mirrors were placed as close as possible to the end-facets of the epitaxy. No index-matching liquid was used.

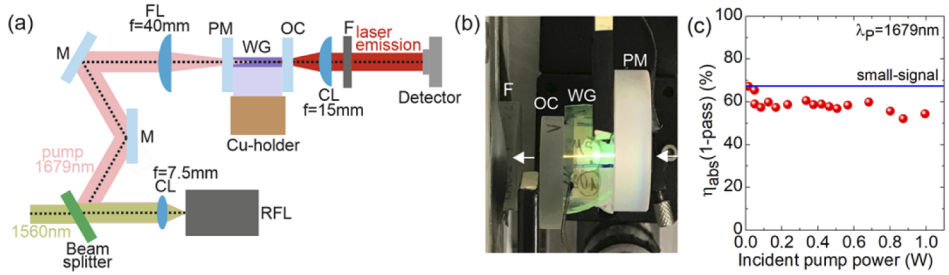

Fig. 3. (a) Scheme of the Tm,Ho waveguide laser: RFL: Raman fiber laser, CL and FL – collimating and focusing lenses, respectively, M: folding mirrors, PM: pump mirror, OC: output coupler, F: filter (a dichroic mirror); (b) Photograph of the pumped WG; (c) Measured single-pass pump absorption as a function of the incident pump power (*circles*), calculated small-signal absorption (*line*).

As a pump source, we employed a home-made Raman fiber laser (RFL) based on an Er fiber master oscillator power amplifier and a single-mode polarization maintaining germanosilicate fiber [16]. The RFL delivered up to 3.5 W at 1679 nm (emission bandwidth: <1 nm) with linear

Optics EXPRESS

polarization and a beam quality factor $M^2 \approx 1$. The selected pump wavelength well matched the maximum of the $^3H_6 \rightarrow {}^3F_4$ absorption band of Tm^{3+} ions in $LiYF_4$, cf. Figure 1(b). The output of the RFL was first collimated using an AR-coated spherical lens (f = 7.5 mm) and then focused at the input facet of the WG using an uncoated CaF_2 lens (f = 40 mm) resulting in a measured pump spot diameter $2w_P$ of 30 ± 5 μm. A photograph of the pumped WG is shown in Fig. 3(b). It shows green-yellow upconversion luminescence of Ho^{3+} ions.

The pump polarization corresponded to σ (TE) in the layer. Although it led to lower absorption cross-section as compared to π-polarization, Fig. 1(b), the use of σ-polarized pump ensured more uniform pump distribution through the whole length of the WG. Previously, this was found to be critical for optimization of Tm,Ho waveguide lasers as for relatively long WGs, unpumped regions act as sources of strong reabsorption losses. In our previous work [8], we intentionally detuned the pump wavelength from the absorption peak. In the present paper, the pump wavelength was fixed, and the polarization state of the pump radiation was changed to fit the σ polarization in the layer.

The pump coupling efficiency $\eta_{coupl} = 91.1\%$ was estimated from the geometrical overlap of the pump beam and the layer, as well as the Fresnel loss. The single-pass pump absorption was determined in a pump-transmission experiment, Fig. 3(c). A certain absorption saturation due to the ground-state bleaching was detected, as η_{abs}(1-pass) slowly decreased from the small-signal absorption, $\eta_{abs,0} = 1 - \exp(-\sigma_{abs}{}^P N_{Tm} t) = 67.4\%$, where $\sigma_{abs}{}^P = 0.23\times10^{-20}$ cm^2. All the OCs provided a reflectivity at ~1.68 μm, so that the pumping was in double-pass. The total (2-pass) pump absorption taken at the threshold pump power slightly decreased with T_{OC}, in the range 76.8% - 68.9%.

The laser output was separated from the residual (non-absorbed) pump using a long-pass filter (a dichroic mirror). The spectra of laser emission were measured by an optical spectrum analyzer (Yokogawa, model AQ6375B). The mode profile at the output facet of the WG was captured using a short focal length CaF_2 lens (f = 15 mm) and a FIND-R-SCOPE near-IR camera. A scale calibration for the camera was provided by illuminating the epitaxy with near-IR light revealing the layer with a known thickness.

3. Waveguide laser performance

The Tm,Ho:$LiYF_4$ waveguide laser operating in the CW regime generated a maximum output power of 540 mW at 2051 nm with a slope efficiency η of 32.6% (vs. the absorbed pump power), a laser threshold of 337 mW and a maximum optical-to-optical conversion efficiency η_{opt} of 26.3% (vs. the pump power incident on the WG) by using an output coupler with $T_{OC} = 20\%$, see Fig. 4(a). For higher output coupling, the laser performance deteriorated probably due to higher losses related by enhanced ETU. With increasing T_{OC}, the laser threshold gradually increased from 143 mW (0.5% OC) to 473 mW (30% OC). The input-output dependences were linear, and no signs of thermal roll-over was observed. Further power scaling was limited by the available pump power. No damage of the waveguide nor cavity mirrors was observed.

The typical spectra of laser emission are shown in Fig. 4(b). The waveguide laser operated solely on the $^5I_7 \rightarrow {}^5I_8$ Ho^{3+} transition and no Tm^{3+} colasing was observed. The laser polarization was linear (π); it was naturally selected by the gain anisotropy, Fig. 5(a). For small output coupling (T_{OC} = 1.5% - 3%), the laser emission was observed around two wavelengths, 2052 and 2065 nm. For higher $T_{OC} \geq 5\%$, the laser operated only around 2051 nm. This behavior is due to the quasi-three-level nature of the Ho^{3+} laser scheme with reabsorption and it agrees with the gain spectra of Ho^{3+} ions in $LiYF_4$ (see below).

The propagation losses in the Tm,Ho:$LiYF_4$ WG were evaluated by the Caird method [17], Fig. 4(c), i.e., by fitting the dependence of the inverse of the slope efficiency, $1/\eta$, on the inverse of the output-coupling loss, $1/\gamma_{OC}$, using the formula $(1/\eta) = (1/\eta_0)[1 + 2(\gamma/\gamma_{OC})]$, where $\gamma = -\ln(1 - L)$, L is the passive loss per pass, $\gamma_{OC} = -\ln(1 - T_{OC})$, and η_0 is the intrinsic slope efficiency.

Optics EXPRESS

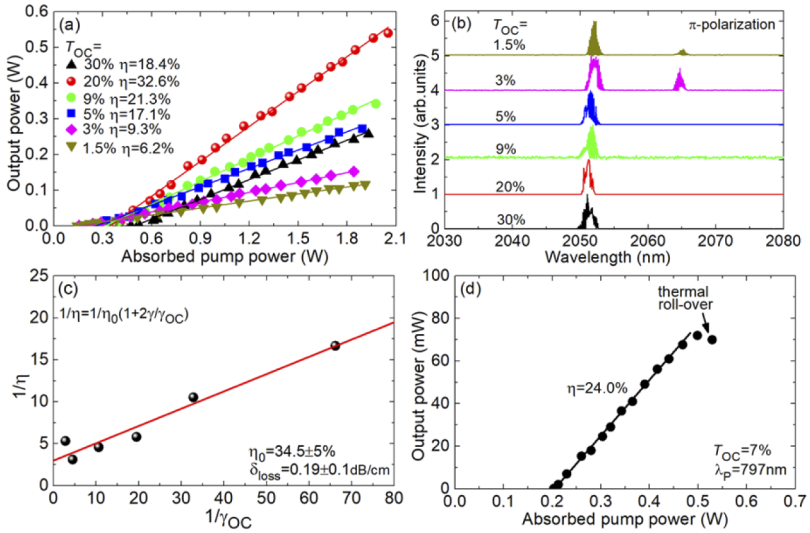

Fig. 4. Output performance of the in-band pumped Tm,Ho:$LiYF_4$ waveguide laser: (a) input-output dependences, η – slope efficiency; (b) typical spectra of laser emission (π-polarization); (c) evaluation of the propagation losses δ_{loss} using the Caird plot; (d) output performance of the same WG under conventional pumping ($\lambda_P = 797$ nm), $T_{OC} = 7\%$.

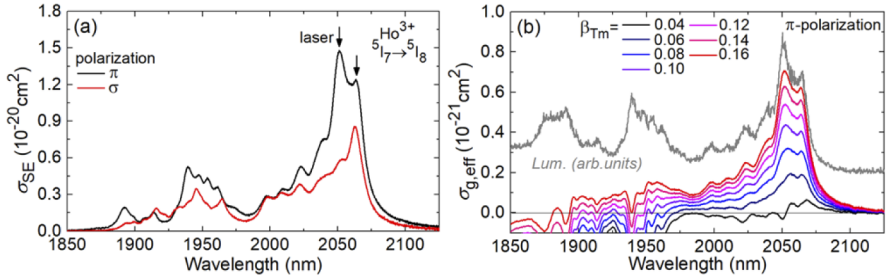

Fig. 5. (a) Stimulated-emission (SE) cross-section, σ_{SE}, spectra for the $^5I_7 \rightarrow {}^5I_8$ transition of Ho^{3+} ions in $LiYF_4$ for π and σ polarizations; (b) effective gain cross-section, $\sigma_{g,eff}$, profiles for a 4.5 at.% Tm, 0.5 at.% Ho codoped $LiYF_4$ crystal for π-polarization, $\beta_{Tm} = N(^3F_4)/N_{Tm}$ is the inversion ratio for Tm^{3+} ions, *grey curve* – the luminescence spectrum from the epitaxy.

The best-fit parameters are $\eta_0 = 34.5 \pm 5\%$ and L corresponding to the WG propagation loss $\delta_{loss} = 0.19 \pm 0.1$ dB/cm. This value is close to ones reported previously for Yb:$LiYF_4$ (0.2 dB/cm at ~1 μm) [18] and Tm:$LiYF_4$ (0.11 dB/cm at ~1.9 μm) [19] planar waveguides produced by LPE.

For comparison, we studied the output performance of the same WG under conventional pumping employing a Ti:Sapphire laser tuned to 797 nm, Fig. 4(d). CW operation was achieved with the highest output coupling of 7% and the laser generated only 72 mW at 2051 nm with $\eta = 24.0\%$ and a laser threshold of 203 mW. A thermal roll-over was observed for an absorbed pump power >0.5 W and the laser ceased at > 0.55 W. This clearly proved better power scaling capabilities with the in-band pumping scheme.

To explain the observed spectral behavior of the Tm,Ho waveguide laser, the so-called effective gain cross-section, $\sigma_{g,eff}$, spectra [20] were calculated, Fig. 5(b). They account for both the

Optics EXPRESS

absorption and stimulated emission of Tm^{3+} and Ho^{3+} ions around 2 μm, and a bidirectional energy transfer between them, $Tm^{3+}(^3F_4) \leftrightarrow Ho^{3+}(^5I_7)$, leading to equilibrium populations of the excited multiplets [21]. For small inversion ratios for Tm^{3+} ions $\beta_{Tm} < 0.05$, a peak at 2065 nm is observed in the spectra. For intermediate $0.05 < \beta_{Tm} < 0.08$, almost equal gain is observed at 2051 nm and 2065 nm. For large $\beta_{Tm} > 0.08$, the former peak dominates. This agrees with the spectral behavior of the Tm,Ho WG laser considering that higher output coupling loss implies higher inversion in the gain medium. Figure 5(b) also confirms that there is no possibility for Tm^{3+} colasing at ~1.9 μm due to the reabsorption loss induced by Ho^{3+} ions in this spectral range.

The laser mode profile at the output waveguide facet is shown in Fig. 6(a). It has a horizontal stripe shape which is typical for planar waveguide lasers. The 1D intensity profiles in the horizontal (x) and vertical (y, || $\boldsymbol{c}$-axis) directions are shown in Fig. 3(b). The mode size (at the $1/e^2$ level) is 310 (x) × 24 (y) μm^2. The intensity profile along the y-axis is close to the Gaussian one, while a strongly multimode behavior is observed along the x-axis.

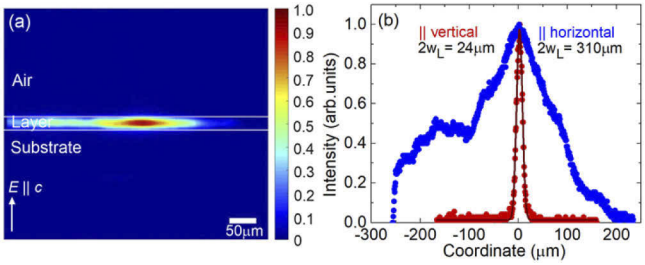

Fig. 6. Mode profile at the output facet of the Tm,Ho:$LiYF_4$ waveguide laser: (a) 2D profile, while lines mark the layer / substrate and the layer / air interfaces; (b) 1D intensity profiles in the horizontal (x) and vertical (y) directions. *Dark-red curve* – Gaussian fit of the intensity profile (vertical direction). The laser polarization (π) is vertical.

In Table 1, we compare the output characteristics of Tm,Ho waveguide lasers reported so far. In this work, we report on the highest output power and slope efficiency achieved from any Tm,Ho waveguide laser. Moreover, no parasitic Tm^{3+} colasing was observed even for high output coupling, an effect which limited the laser efficiency in the previous studies [6,15].

Table 1. An Overview of Tm,Ho Waveguide Lasers Reported So Far[a]

Method	Type	Material	Doping, at.%	λ_P, nm	P_{out}, mW	λ_L, nm	η, %	P_{th}, mW	Ref.
DLW	channel	glass	1.96 Tm, 0.22 Ho	790	76	2052	20	20	[6]
LPE	planar	$KY(WO_4)_2$	5 Tm, 0.5 Ho	794	1.9	2051	10.5	~2	[7]
LPE	planar	$LiYF_4$	4.5 Tm, 0.5 Ho	797	81	2051	24	200	[8]
DLW	channel	$KLu(WO_4)_2$	5 Tm, 0.5 Ho	1679	144	2059	12.5	206	[15]
LPE	planar	$LiYF_4$	4.5 Tm, 0.5 Ho	1679	**540**	2051	**32.6**	337	[b]

[a] λ_P and λ_L – pump and laser wavelengths, respectively, P_{out} – output power, η – slope efficiency, P_{th} – laser threshold, δ_{loss} - waveguide propagation loss.
[b] This work.

4. Conclusion

To conclude, in-band pumping of Tm^{3+},Ho^{3+}-codoped laser materials (in particular, optical waveguides) is a promising approach for efficient and power-scalable operation above 2 μm

Optics EXPRESS

according to the $^5I_7 \rightarrow {}^5I_8$ Ho^{3+} transition. In the present work, we report on the record-high output power from any Tm,Ho WG laser without any parasitic Tm^{3+} colasing. Further improvement of the laser efficiency is expected in the channel waveguide geometry owing to the better overlap of the pump and laser modes. Considering the combined gain profiles from both Tm^{3+} and Ho^{3+} ions and the location of the gain maximum >2 μm thus avoiding the structured water vapor absorption in the atmosphere, in-band pumped Tm,Ho WGs are promising for generation of ultrashort pulses at high repetition rates from mode-locked oscillators.

Funding. Région Normandie (NOVAMAT, Chaire d'excellence "RELANCE").

Disclosures. The authors declare no conflicts of interest.

Data availability. Data underlying the results presented in this paper are not publicly available at this time but may be obtained from the authors upon reasonable request.

References

1. E. Kifle, P. Loiko, C. Romero, J. R. V. de Aldana, M. Aguiló, F. Díaz, P. Camy, U. Griebner, V. Petrov, and X. Mateos, "Watt-level ultrafast laser inscribed thulium waveguide lasers," Prog. Quantum Electron. **72**, 100266 (2020).
2. R. Mary, G. Brown, S. J. Beecher, F. Torrisi, S. Milana, D. Popa, T. Hasan, Z. Sun, E. Lidorikis, S. Ohara, A. C. Ferrari, and A. K. Kar, "1.5 GHz picosecond pulse generation from a monolithic waveguide laser with a graphene-film saturable output coupler," Opt. Express **21**(7), 7943–7950 (2013).
3. C. Kerse, H. Kalaycıoğlu, P. Elahi, B. Çetin, D. K. Kesim, Ö. Akçaalan, S. Yavaş, M. D. Aşık, B. Öktem, H. Hoogland, and R. Holzwarth, "Ablation-cooled material removal with ultrafast bursts of pulses," Nature **537**(7618), 84–88 (2016).
4. G. L. Bourdet and G. Lescroart, "Theoretical modeling and design of a Tm, Ho:$YLiF_4$ microchip laser," Appl. Opt. **38**(15), 3275–3281 (1999).
5. P. Loiko, J. M. Serres, X. Mateos, K. Yumashev, N. Kuleshov, V. Petrov, U. Griebner, M. Aguiló, and F. Díaz, "Microchip laser operation of Tm,Ho:$KLu(WO_4)_2$ crystal," Opt. Express **22**(23), 27976–27984 (2014).
6. D. G. Lancaster, S. Gross, H. Ebendorff-Heidepriem, A. Fuerbach, M. J. Withford, and T. M. Monro, "2.1 μm waveguide laser fabricated by femtosecond laser direct-writing in Ho^{3+}, Tm^{3+}:ZBLAN glass," Opt. Lett. **37**(6), 996–998 (2012).
7. C.V. Ruiz Madroñero, X. Mateos, P. Loiko, V. Petrov, U. Griebner, M. Aguiló, and F. Díaz, "Tm,Ho:$KY(WO_4)_2$ planar waveguide laser," Laser Phys. Lett. **13**(9), 095801 (2016).
8. P. Loiko, R. Soulard, G. Brasse, J.-L. Doulan, A. Braud, A. Tyazhev, A. Hideur, and P. Camy, "Tm,Ho:$LiYF_4$ planar waveguide laser at 2.05 μm," Opt. Lett. **43**(18), 4341–4344 (2018).
9. O. Antipov, A. Novikov, S. Larin, and I. Obronov, "Highly efficient 2 μm CW and Q-switched Tm^{3+}:Lu_2O_3 ceramics lasers in-band pumped by a Raman-shifted erbium fiber laser at 1670 nm," Opt. Lett. **41**(10), 2298–2301 (2016).
10. P. Loiko, R. Thouroude, R. Soulard, L. Guillemot, G. Brasse, J.-L. Doualan, B. Guichardaz, A. Braud, A. Hideur, M. Laroche, H. Gilles, and P. Camy, "In-band pumping of Tm:$LiYF_4$ channel waveguide: A power scaling strategy for ~2 μm waveguide lasers," Opt. Lett. **44**(12), 3010–3013 (2019).
11. S. McDaniel, F. Thorburn, A. Lancaster, R. Stites, G. Cook, and A. Kar, "Operation of Ho:YAG ultrafast laser inscribed waveguide lasers," Appl. Opt. **56**(12), 3251–3256 (2017).
12. E. Kifle, P. Loiko, C. Romero, J. R. V. de Aldana, A. Ródenas, V. Zakharov, A. Veniaminov, M. Aguiló, F. Díaz, U. Griebner, V. Petrov, and X. Mateos, "Femtosecond-laser-written Ho:$KGd(WO_4)_2$ waveguide laser at 2.1 μm," Opt. Lett. **44**(7), 1738–1741 (2019).
13. Z. Pan, P. Loiko, Y. Wang, Y. Zhao, H. Yuan, X. Dai, H. Cai, J. M. Serres, S. Slimi, E. Dunina, A. Kornienko, J.-L. Doualan, P. Camy, U. Griebner, V. Petrov, M. Aguiló, F. Díaz, and X. Mateos, "Disordered Tm^{3+},Ho^{3+}-codoped CNGG garnet crystal: Towards efficient laser materials for ultrashort pulse generation at ~2 μm," J. Alloys Compd. **853**, 157100 (2021).
14. Y. L. Kalachev, V. A. Mikhailov, V. V. Podreshetnikov, and I. A. Shcherbakov, "Study of a Tm:Ho:YLF laser pumped by a Raman shifted erbium-doped fibre laser at 1678 nm," Quantum Electron. **40**(4), 296–300 (2010).
15. E. Kifle, P. Loiko, C. Romero, J. R. V. de Aldana, V. Zakharov, Y. Gurova, A. Veniaminov, V. Petrov, U. Griebner, R. Thouroude, M. Laroche, P. Camy, M. Aguiló, F. Díaz, and X. Mateos, "Tm^{3+} and Ho^{3+} colasing in in-band pumped waveguides fabricated by femtosecond laser writing," Opt. Lett. **46**(1), 122–125 (2021).
16. R. Thouroude, H. Gilles, B. Cadier, T. Robin, A. Hideur, A. Tyazhev, R. Soulard, P. Camy, J-L. Doualan, and M. Laroche, "Linearly-polarized high-power Raman fiber lasers near 1670 nm," Laser Phys. Lett. **16**(2), 025102 (2019).
17. J. A. Caird, S. A. Payne, P. R. Staber, A. J. Ramponi, L. L. Chase, and W. F. Krupke, "Quantum electronic properties of the $Na_3Ga_2Li_3F_{12}$:Cr^{3+} laser," IEEE J. Quantum Electron. **24**(6), 1077–1099 (1988).
18. W. Bolaños, F. Starecki, A. Braud, J.-L. Doualan, R. Moncorgé, and P. Camy, "2.8 W end-pumped Yb^{3+}:$LiYF_4$ waveguide laser," Opt. Lett. **38**(24), 5377–5380 (2013).
19. W. Bolanos, F. Starecki, A. Benayad, G. Brasse, V. Ménard, J.-L. Doualan, A. Braud, R. Moncorgé, and P. Camy, "Tm:$LiYF_4$ planar waveguide laser at 1.9 μm," Opt. Lett. **37**(19), 4032–4034 (2012).

Optics EXPRESS

20. Z. Pan, P. Loiko, Y. Wang, Y. Zhao, H. Yuan, K. Tang, X. Dai, H. Cai, J. M. Serres, S. Slimi, E. B. Salem, E. Dunin, A. Kornienko, L. Fomicheva, J.-L. Doualan, P. Camy, W. Chen, U. Griebner, V. Petrov, M. Aguiló, F. Díaz, R. M. Solé, and X. Mateos, "Disordered Tm^{3+},Ho^{3+}-codoped CNGG garnet crystal: Towards efficient laser materials for ultrashort pulse generation at ~2 μm," J. Alloys Compd. **853**, 157100 (2021).
21. B. M. Walsh, N. P. Barnes, and B. Di Bartolo, "The temperature dependence of energy transfer between the Tm $^3F_4$ and Ho $^5I_7$ manifolds of Tm-sensitized Ho luminescence in YAG and YLF," J. Lumin. **90**(1-2), 39–48 (2000).